



Clustering behavior in a three-layer system mimicking olivo-cerebellar dynamics

Manuel G. Velarde^{a,b,*}, Vladimir I. Nekorkin^{a,c}, Valeri A. Makarov^a,
Vladimir I. Makarenko^d, Rodolfo R. Llinás^d

^a*Instituto Pluridisciplinar, Universidad Complutense, Paseo Juan XXIII, No 1, Madrid 28 040, Spain*

^b*International Center for Mechanical Sciences (CISM), Palazzo del Torso, Piazza Garibaldi, Udine 33100, Italy*

^c*Radiophysical Department, Nizhny Novgorod State University, Gagarin Avenue, No 23, Nizhny Novgorod 603600, Russian Federation*

^d*Department of Physiology and Neuroscience, New York University School of Medicine, 550 First Ave., New York, NY 10016, USA*

Received 10 January 2002; accepted 9 July 2003

Abstract

A model is presented that simulates the process of neuronal synchronization, formation of coherent activity clusters and their dynamic reorganization in the olivo-cerebellar system. Three coupled 2D lattices dealing with the main cellular groups in this neuronal circuit are used to model the dynamics of the excitatory feedforward loop linking the inferior olive (IO) neurons to the cerebellar nuclei (CN) via collateral axons that also proceed to terminate as climbing fiber afferents to Purkinje cells (PC). Inhibitory feedback from the CN-lattice fosters decoupling of units in a vicinity of a given IO neuron. It is shown that noise-sustained oscillations in the IO-lattice are capable to synchronize and generate coherent firing clusters in the layer accounting for the excitable collateral axons. The model also provides phase resetting of the oscillations in the IO-lattices with transient silent behavior. It is also shown that the CN–IO feedback leads to transient patterns of couplings in the IO and to a dynamic control of the size of clusters.

© 2003 Elsevier Ltd. All rights reserved.

Keywords: Inferior olive; Dynamical clusters; Noise; Neuron ensemble oscillations; Nonlinear dynamics

1. Introduction

In vitro and in vivo experiments have shown that inferior olive neurons (IO) possess intrinsic mechanisms, which endow them with complex functional properties (Armstrong, Eccles, Harvey, & Matthews, 1968; Bal & McCormick, 1997; Bell & Kawasaki, 1972; Benardo & Foster, 1986; Bower & Llinas, 1982; Fukuda, Yamamoto, & Llinas, 1987; Lampl & Yarom, 1997; Llinas & Sasaki, 1989; Llinas & Volkind, 1973; Llinas & Yarom, 1981 a,b; Sasaki, Bower, & Llinas, 1989; Sasaki & Llinas, 1985). On the one hand, these neurons can behave as autonomous oscillators, and, on the other hand, as a neuronal ensemble producing synchronous spikes. These are then transmitted through axons, the climbing fibers afferent to the Purkinje cell (PC) array (Szentagothai & Rajkovits, 1959) and with

collaterals to the cerebellar nuclei (CN) (Chan-Palay & Palay, 1971). In turn, CN neurons send inhibitory terminals to the IO (Nelson, Barmack, & Mugnaini, 1984; Ruigrok, 1997) (see Fig. 1A). Furthermore, because the terminals are situated mostly on the gap junctions coupling IO cells (Sotelo, Gotow, & Wassef, 1986), it has been proposed that such a return pathway serves as a feedback inhibitory, decoupling signal to IO neurons, creating conditions for varying, evolving multi-cluster activity, hence time-changing pools of synchronously oscillating neurons (Llinas, 1989; Llinas, Baker, & Sotelo, 1974; Mugnani & Oertel, 1981; Sotelo, Llinas, & Baker, 1974). Note that about half of the CN cells are GABAergic and project directly to the IO. The data suggest that the GABAergic modulation of electrotonic coupling is a mechanism that is fundamental to the function of the olivo-cerebellar system in all mammals (Gottlieb, 1988).

Although neurons in different regions of the IO may have different oscillatory properties, three main conductances, in addition to those leading to action potentials, have been

* Corresponding author. Address: Instituto Pluridisciplinar, Universidad Complutense, Paseo Juan XXIII, No 1, Madrid 28 040, Spain. Tel.: +34-91-3943242; fax: +34-91-3943243.

E-mail address: velarde@fluidos.pluri.ucm.es (M.G. Velarde).

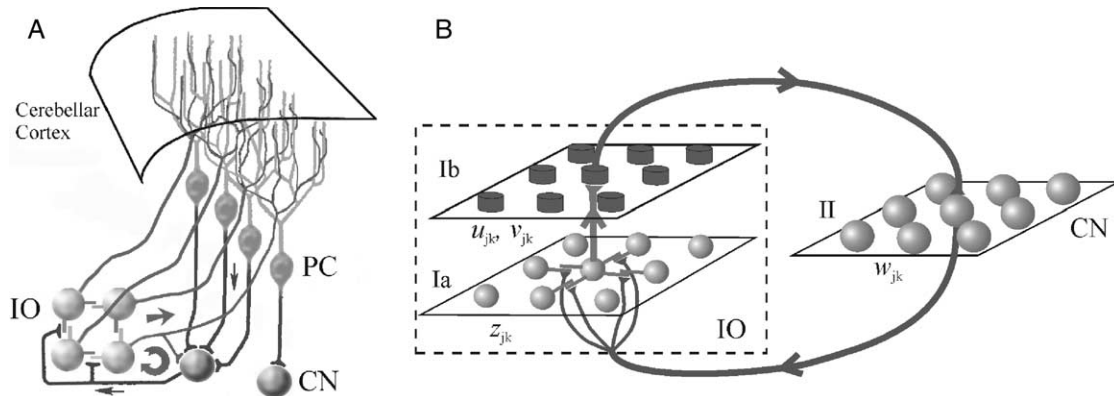


Fig. 1. (A) Schematic organization of the Olivo-Cerebellar system including its three major components: inferior olive (IO), purkinje cell array (PC), and cerebellar nuclei (CN) where two autonomous loops IO–PC–CN and IO–CN are displayed. (B) A three-layer system that in the simplest possible terms depicts the most significant features from (A) and hence mimics the overall dynamics of the Olivo-Cerebellar system. It contains oscillatory (lattice Ia, somatic subthreshold oscillations) and excitatory (lattice Ib, axonal action potentials) features of the IO neurons and the output of signal processing in the CN layer (lattice II) feeding back to IO. A sphere from Ia and a tube-like unit from Ib account for an IO neuron. Intra-layer couplings in the lattice Ia (only couplings of the central unit are shown) describe dendritic gap junction couplings between IO neurons. Note that the arrowed feedforward I-II interlayer connection (illustrated with coupling between central units only) accounts in global way for the main effect of the two loops in part A of the figure. No interactions between units in lattices Ib and II are considered as experimental data suggest (part A is redrawn from Llinas & Welsh, 1993).

advocated to be responsible for the oscillatory properties of IO neurons: a dendritic high-threshold Ca^{2+} conductance, a somatic low-threshold Ca^{2+} conductance, and a Ca^{2+} -activated K^+ conductance (Llinas & Yarom, 1981a,b; Manor, Rinzel, Segev, & Yarom, 1997). Furthermore, the interaction of the high-threshold Ca^{2+} current and the Ca^{2+} -activated K^+ current has been proposed to account for the generation of low (up to 6 Hz) firing frequency whereas higher (up to 10 Hz) firing frequency is thought to occur at more hyperpolarized potentials with less involvement of the high-frequency Ca^{2+} current. Indeed, the Ca^{2+} -dependent K^+ conductance (150–200 ms duration) inhibits firing at frequencies above 6 Hz. If, however, the membrane potential is shifted to more and more negative values, hence further hyperpolarized, allowing the activation of the high-threshold spike, the duration of the hyperpolarization is shortened and the neuron can respond at frequencies of up to 10 Hz.

Synchronous oscillation of IO neurons appears as significant in timing and dynamic organization of motor sequences in motor coordination (Llinas, 1989; Fukuda, Yamamoto, & Llinas, 2001; Llinas & Sasaki, 1989; Llinas & Welsh, 1993; Vallbo & Wessberg, 1993; Welsh, Lang, Sugihara, & Llinas, 1995; Welsh & Llinas, 1997; Yamamoto, Fukuda, & Llinas, 2001). Multi-electrode experiments with PCs in the rodent cerebellar cortex (Llinas & Sasaki, 1989; Sasaki et al., 1989) have also shown that the number of cells participating in isochronous spike clusters is relatively small for spontaneous activity and increases with neuropharmacological intervention with drugs such as harmaline or picrotoxin (Lang, Sugihara, & Llinas, 1996; Llinas & Sasaki, 1989; Llinas & Yarom, 1986). Harmaline is a tremorgenic drug. Indeed, when harmaline is administered in vivo, it results in a 10 Hz tremor due to the induction of oscillatory behavior in the IO (Lamarre et al.,

1971; Llinas & Volkind, 1973; de Montigny & Lamarre, 1973). Harmaline tends to hyperpolarize the membrane and increases the voltage sensitivity of the low threshold calcium current (Llinas & Yarom, 1986), hence allowing the aforementioned relative high-firing frequency. Harmaline has also been shown blocking the time-dependent inward rectification (sag) (Yarom & Llinas, 1987). Picrotoxin is a GABAergic antagonist and it has been shown that injection of picrotoxin modulates the level of the electrotonic coupling among IO neurons increasing the size of IO neuron clusters by partially merging smaller clusters into larger areas of activation (Lang et al., 1996). Neurons in different regions of the IO show differing sensitivities to picrotoxin. Picrotoxin injection has also been shown to increase the rate of spontaneous complex spikes to nearly twice control levels, on average, with also an increase of synchronicity and rhythmicity of such complex spike activity (Yamamoto et al., 2001). Blocking the GABAergic inhibitory connection within the IO glomeruli, where the gap junctions are located, allows IO neuron clusters to grow bigger increasing the electrical load of the network and within clusters (Lang et al., 1996). The modulation of the electrotonic coupling provides means for an external stimulus to control the sensitivity of the loops IO–PC–CN and IO–CN. Such modulations allow the formation of well-organized patterns of global activity, which are of significance in motor coordination (Welsh, Lang, Sugihara, & Llinas, 1995). The patterns evolve in time as the autonomous excitatory-inhibitory loops suitable to recognize the clusters of synchronous firing neurons and prevent their uncontrolled growth. The clusters in the IO generally reorganize as the amplitudes decay with subsequent phase resetting (Makarenko & Llinas, 1998). Details about synchronization, clustering and related phase resetting phenomena for various nonlinear oscillator models can be

found in the literature (Haken, 1996; Hoppensteadt, 1986; Mikhailov & Calenbuhr, 2002; Nekorkin & Velarde, 2002; Tass, 1999).

Recently, several models accounting for structural and functional levels of IO neurons have been proposed (Giaquinta, Argentina, & Velarde, 2000; Manor et al., 1997; Schweighofer, Doya, & Kawato, 1999; Velarde, Nekorkin, Kazantsev, Makarenko, & Llinas, 2002). For instance, Manor et al. (1997) and Schweighofer et al. (1999) use compartmental models and variables based on electrophysiological properties of IO neurons thus clarifying the relations between significant ionic currents and the dynamic behavior of the IO neuron, starting with subthreshold oscillations. Manor et al. (1997) discuss mechanisms underlying subthreshold oscillations using a single compartment Hodgkin–Huxley-like model that includes leakage and low threshold calcium currents. Schweighofer et al. (1999) propose a two-compartment model with nine ionic currents. They were able to obtain good agreement with available experimental data. To describe the behavior of a single neuron all these models either demand consideration of many variables nonlinearly coupled (Schweighofer et al., 1999; Velarde et al., 2002) or a complex nonlinearity to exhibit subthreshold oscillations (Giaquinta et al., 2000; Manor et al., 1997). As our interest in the present study focuses on understanding how collective features may appear and hence we are only interested on simulating the ensemble behavior of IO neurons and the autonomous activity of the Olivo-Cerebellar circuit observable in the absence of external input, details about the specificity of units are not really needed here. It suffices that model IO neurons are able to oscillate, to form clusters, and to send spikes when subthreshold oscillations overcome a certain threshold value. Reducing complexity in the model of a single neuron is expected to allow transparency in the understanding of the behavior of neuron clusters and the dynamics of the overall process in the cerebellar functional loop. Accordingly, we shall consider the following simplifications. To a first approximation, enough for the earlier mentioned scope of this work, the gap junctions are reduced to just nearest-neighbor diffusive (electrical) couplings (bonds). We shall not consider the details of the process of propagation of the action potentials via axons. Given that signal propagation is very fast (time delay is less than 3% of the base oscillation period (Sugihara, Lang, & Llinas, 1993)), the time intervals for transferring a spike from IO neurons to CN are similar for all connections (Sugihara et al., 1993) and hence negligible.

The paper is organized as follows. In Section 2 we outline the simplest mathematical model that adequately mimics oscillations, synchronization and desynchronization processes, clustering in the IO ensemble and the minimal significant representation of the overall dynamics depicted in Fig. 1A. A schematic diagram of the model is shown in Fig. 1B. It involves three different, interconnected two-dimensional lattices. The two-layer block IO accounts for

the oscillatory (somatic subthreshold oscillations in lattice Ia) and excitatory (axon spiking in lattice Ib) features of the IO neurons, taken separately for purposes of mathematical description. Hence a sphere in lattice Ia combined with its corresponding tube in lattice Ib mimics the dynamics of an IO neuron in full. In fact, such apparently artificial separation in two parts is suggested by the experimental data. The gap junctions between IO cells are mostly located on the dendrites (Llinas et al., 1974; Sotelo et al., 1974). The feedforward coupling (arrow) that leads to lattice II is associated with the loop IO–CN. One may assume that in the absence of external input this loop is taken functionally accounting for both the PC-mediated and the direct IO–CN connections. The loop finally feeds back the IO lattice and modulates the diffusive intra-layer bonds (gap junctions) in the vicinity of a given neuron in Ia. Section 3 is devoted to the study of the model in the particular case when couplings in lattice Ia are of constant value. This choice of parameter value mimics well the earlier mentioned consequence of injecting picrotoxin into the IO and/or lesions of the CN nucleus (Lang et al., 1996) in in vivo experiments that reduce the GABAergic CN–IO inhibitory feedback loop. In Section 4 we take up the general case and consider the action of the feedback loop on the cluster activity of the IO system. Thus we discuss in our mathematical model features that resemble what in reality would be the influence of increasing low threshold calcium conductance and neuron hyperpolarization (using harmaline) on the coherence of spike trains (Lang et al., 1996; Llinas & Sasaki, 1989). In Section 5 we summarize our results.

2. The model

Following the scheme shown in Fig. 1B let us now construct a mathematical model simulating the cooperative, functional behavior of the cerebellar loop. According to experimental data the IO neurons go through low amplitude (about 5 mV) subthreshold oscillations with well-defined frequency (about 10 Hz in vivo) and, eventually, fire spikes when the threshold voltage is attained (Llinas & Yarom, 1986). The frequency of spikes can change from 1 to 10 Hz (Latham & Paul, 1971). The simplest possible oscillator one can think about is a harmonic one. Although it does not possess robust oscillations like limit cycle behavior in a nonlinear system (Cronin, 1987; Giaquinta et al., 2000; Hoppensteadt, 1986; Izhikevich, 2000; Manor et al., 1997; Schweighofer et al., 1999; Velarde et al., 2002) it suffices for our purpose here. Indeed, as neurons are always subjected to noise (intrinsic or arising from the medium) we could consider a harmonic oscillator with added noise and then it is known that when oscillations exist they are robust (Holden, 1976; Tuckwell, 1989). A similar consequence occurs when a time delay is added to a harmonic oscillator that helps to establish limit cycle oscillations (Campbell, Belair, Ohira, & Milton, 1995; MacDonald,

1989; Olien & Belair, 1997; Wei, Verlade, & Makarov, 2002). Thus adding noise to such an oscillator we obtain sustained oscillations. Noise can be introduced in the system in different ways. Here, for simplicity, we restrict consideration to the case of an additive Gaussian noise (Doi, Inpue, Sato, & Smith, 1999; Gardiner, 1985; Manganaro, Arena, & Fortuna, 1999; Tuckwell, 1989). A more realistic multiplicative, eventually colored noise would add difficulties that will eliminate transparency in the main features that the noise can bring. Thus for the IO part responsible of subthreshold oscillations we take a two-dimensional ($n \times n$) lattice (lattice Ia in Fig. 1B) where at each site (jk) we have

$$\dot{z}_{jk} = z_{jk}(i\omega_0 - \gamma) + i\sqrt{2D}\xi_{jk}(t). \quad (1a)$$

The quantity z is a complex variable characterizing the dynamics of a neuron (if only the real part is used, say, x , then Eq. (1a) would transform into the standard form of a harmonic oscillator with second derivative in time; a dot over a quantity denotes time derivative), γ is a damping constant, ω_0 is the angular oscillation frequency in the absence of noise and damping ($\omega_0 = 2\pi \times 10$ Hz), $\xi_{jk}(t)$ are zero mean independent noise sources with a time correlation function given by

$$\langle \xi_{lm}(t)\xi_{jk}(t') \rangle = \delta_{(jk)(lm)}\delta(t - t'),$$

and D is a parameter, which sets the noise intensity. As earlier announced, in the absence of noise, $D = 0$, oscillations decay in time (even in the presence of passive, e.g. electrical gap junction-like bonds between oscillators), while for nonzero noise we have self-sustained oscillations. Gap junctions are described by electrical resistors, diffusive-like bonds between units in the lattice Ia (Fig. 1B)

$$\dot{z}_{jk} = z_{jk}(i\omega_0 - \gamma) + i\sqrt{2D}\xi_{jk}(t) + \sum_{lm \in L} d_{jk}^{lm}(z_{lm} - z_{jk}), \quad (1b)$$

where d_{jk}^{lm} accounts for the value of the coupling or bond strength between neurons at sites (jk) and (lm). As mentioned earlier its actual value is affected (via feedback) by the dynamics of the CN lattice. We shall return to this problem later when we describe the dynamics of CN. Eq. (1b) is considered with periodic boundary conditions, thus disregarding the influence of boundaries on the dynamics of the system. The sum in the right part of Eq. (1b) is taken over neighboring neurons

$$L : (l - j)^2 + (m - k)^2 \leq R^2, \quad (2)$$

where R accounts for the radius of neuron interaction. The simplest nearest-neighbor coupling implies $R = 1$. Further on we shall consider only this case, as this choice of parameter value does not affect the generality of the results obtained with the model.

The lattice (1b) is expected to produce oscillations with a narrow frequency band peaked around ω_0 with relatively slowly varying amplitudes. These oscillations are

the external input for the second ($n \times n$) lattice (Ib in Fig. 1B) consisting of excitable, FitzHugh–Nagumo (Fitz Hugh, 1961; Hoppensteadt, 1986) elements

$$\varepsilon \dot{u}_{jk} = f(u_{jk}) - v_{jk}, \quad \dot{v}_{jk} = u_{jk} - I_{jk}(t), \quad (3)$$

where $\varepsilon \ll 1$ is a small parameter; u_{jk} and v_{jk} mimic, respectively, voltage and recovery variables of the axon-like unit in the corresponding site of layer Ib. We take the nonlinear function, $f(u)$, in the form of a polynomial

$$f(u) = \alpha u^2 \left(-\frac{1}{5}u^3 + \frac{a^2}{6}u - \frac{a^3}{4} \right). \quad (4)$$

The parameters a and α allow us to tune amplitude and duration of a pulse, respectively. For $\varepsilon = 0$ we can formally get the spike amplitude, $A_{sp} = 1.924a$, and its duration $T_{sp} = 0.1327\alpha a^4$, which do not practically change for $\varepsilon \ll 1$. Then we set $a = 2$ and choose α such that $T_{sp} = 4$ ms which is about the duration of an action potential in a collateral axon.

Axons (and PC) in lattice Ib are taken uncoupled and get excitation from layer Ia via the activation current $I_{jk}(t)$ as experiments with IO neurons suggest (Llinas & Welsh, 1993). We consider unidirectional coupling between corresponding elements in lattices Ia and Ib. The current I_{jk} depends on the corresponding variable in the bottom layer in IO (Fig. 1B). The simplest choice for this current is

$$I_{jk}(t) = -I_0 + x_{jk}(t), \quad (5)$$

where $x_{jk} = \text{Re}z_{jk}$ and I_0 is a positive constant dealing with the level of hyperpolarization of IO neurons. The system (3) has its threshold at $I_{jk} = -a$. Consequently, from Eq. (5) we have a threshold value for oscillations in the lattice Ia (Fig. 1B) $x_{th} = I_0 - a$. For $I_{jk} < -a$ there exist only low amplitude oscillations around the rest state (with average membrane potential $\langle u_{jk} \rangle = -I_0$). However, if $I_{jk} > -a$ the variable u_{jk} performs a large excursion to high values and comes back. Thus, the IO neuron produces spikes in Ib with amplitude A_{sp} and duration T_{sp} .

The CN lattice gets excitatory signals from the corresponding axons in lattice Ib and then inhibits couplings (decreasing coupling strength values) in the IO lattice by decreasing IPSP for time intervals about 30 ms. Accordingly, for the CN lattice (lattice II in Fig. 1B) we take

$$\tau \dot{w}_{jk} = -w_{jk} + \Theta(u_{jk}), \quad (6)$$

where w is the variable mimicking the CN response, τ is the time scale of decay, and $\Theta(u)$ is the sigmoidal (Boltzmann) function

$$\Theta(u) = \frac{\exp[10(u + I_0 - 0.6)]}{1 + \exp[10(u + I_0 - 0.6)]}. \quad (7)$$

Without stimulus (the corresponding unit in lattice Ib is at rest, $u_{jk} = -I_0$) $\Theta(u_{jk}) \approx 0$ and, consequently, for system (6) we have $w_{jk} = 0$. Each incoming spike switches-on the function $\Theta(u_{jk})$ for a period T_{sp} . This leads to an almost

linear increase of w_{jk} up to the value T_{sp}/τ and in turn w_{jk} exponentially decays to the rest level. The duration of the resulting pulse, with 0.7 height, is about $\tau \ln \frac{10}{7}$. Thus to have it lasting for approximately 30 ms we set $\tau = 0.08$.

The pulse formed by the variable w reduces the strength of the electrical coupling in the vicinity of a given neuron in the IO lattice (Fig. 1B). Thus for the coupling coefficients, d_{jk}^m , in the system (1b) we can write

$$d_{jk}^m = \frac{1}{1 + \Gamma \sum w_{pq}} d, \quad (8)$$

where d is the maximal coupling strength, i.e. in the absence of feedback loop; Γ accounts for the magnitude of coupling degradation due to the feedback; and summation is taken over units which can destroy the bond $(lm) - (jk)$. In Fig. 1B we assume that decoupling affects only four bonds. Thus, only two neurons, (lm) and (jk) , can destroy the coupling $(lm) - (jk)$.

In addition, the activity of lattice Ib in Fig. 1B reflects the spiking behavior of the PC level and allows us to monitor such activity, since each PC is innervated by one climbing fiber and a single IO spike generates a single ‘complex spike’ in PC (Eccles et al., 1966; Llinas & Simpson, 1981; Yarom, 1989). To visualize spiking activity and the space-time evolution of the system we use ‘raster displays’ (Lang et al., 1996), plotting a small vertical bar for each spiking event occurring in the lattice Ib (Fig. 1B). We shall use this to compare our results to experimental data obtained by multi-electrode recordings from rodent cerebellar cortex (Fukuda et al., 2001; Yamamoto et al., 2001).

3. Response of the excitable elements to subthreshold oscillations in the oscillatory lattice without feedback loop

Let us suppose now that the value of the electrical coupling between IO neurons is constant and does not depend on the dynamics of the CN lattice, $d_{jk}^m = d$ ($\Gamma = 0$). As mentioned earlier such mode can be achieved in experiments by the blockage of GABA with picrotoxin or lesions of the CN (Fukuda et al., 2001; Lang et al., 1996; Yamamoto et al., 2001). Then due to the unidirectional coupling between lattices Ia and Ib in IO (Fig. 1B) we can consider the lattice Ia as a *master* lattice, which *slaves* the second lattice Ib. We expect that the noise will excite oscillations in the units in the master lattice, which are not correlated for $d = 0$, and become more and more correlated with the increase of the coupling coefficient. Consequently, due to the inter-lattice interaction we get spike trains with higher and higher level of coherence.

Let us now investigate how the noise affects the oscillations in the first layer for different values of the coupling, d , and the response of the slaved lattice to such activation. Clearly, for small intensity levels the noise is able to excite only low amplitude oscillations. In the limit of

uncoupled neurons, $d = 0$, we get from Eq. (1b) $n \times n$ independent stochastic differential equations

$$\ddot{x}_{jk} + 2\gamma\dot{x}_{jk} + \Omega_0^2 x_{jk} = \sqrt{2\omega_0 D} \xi_{jk}(t) \quad (9)$$

where $\Omega_0^2 = \omega_0^2 + \gamma^2$. The noise intensity now is proportional to $\omega_0^2 D$. The fluctuation–dissipation theorem (Gardiner, 1985) yields $T = \frac{\omega_0^2 D}{4\gamma}$, where T represents the noise ‘temperature’. The calculation of the power spectrum of the stochastic process defined by Eq. (9), i.e. of the thermal noise, is straightforward

$$S(\omega) = \frac{\omega_0^2 D}{[\omega^2 - (\omega_0^2 + \gamma^2)]^2 + 4\gamma^2 \omega^2}. \quad (10)$$

If $\omega_0 > \gamma$ the power spectrum Eq. (10) has a peak at the frequency $\omega_{\max}^2 = \omega_0^2 - \gamma^2$ with height

$$S(\omega_{\max}) = \frac{D}{4\gamma^2}. \quad (11)$$

When dissipation is small and hence its time constant is much larger relative to the oscillation period, $\gamma \ll \omega_0$, we have a narrow band process or *quasi-monochromatic* noise. The variables x_{jk} perform fast random oscillations at a frequency around ω_0 with slowly varying amplitude. Such oscillations are similar to the subthreshold oscillations observed in IO neurons in vitro, therefore further on we shall use this parameter choice.

Since the oscillators in the lattice (9) are independent, the normalized cross-correlation function

$$C_x(R) = \frac{1}{\sigma_x^2} (\langle x_{jk}(t)x_{lm}(t) \rangle - \langle x \rangle^2) \quad (12)$$

has zero value for all $R > 0$. Here σ_x is the standard deviation of the process $x(t)$ and $R = \sqrt{(j-l)^2 + (k-m)^2}$ is the distance between oscillators at sites (jk) and (lm) . Thus, we can consider only one unit in Eq. (9) (lattice Ia) and its influence on the dynamics of the corresponding unit in the FitzHugh–Nagumo lattice Ib (Eq. (3)). Firing activity of noise-driven excitable systems has been investigated by several authors (Baltanas and Casado, 1998; Lee et al., 1998; Longtin, 1997; Makarov, Nekorkin, & Verlade, 2001; Pikovsky & Kurths, 1997). Baltanas & Casado (1998) have found that a system similar to Eqs. (3) and (9) (one unit has been considered) is capable of generating both spikes and bursts of spikes. Moreover, spike trains reflect the structure of the underlying oscillations. Inter-spike interval histograms (ISIH) show an imperfect phase locking between ISIs and both the period of the fundamental oscillatory component and the time scale of the random modulation. In this section we extend the study to the case of coupled units (via lattice Ia in Fig. 1B). Fig. 2 shows an example of the time realization of the stochastic process, $x(t)$, its power spectrum and the response of the corresponding units in the Axon (Ib) and CN (II) lattices. The spectrum of the process $x(t)$ has a well-defined peak at the frequency 10 Hz. In the axon $[u(t)]$ we have narrow spiking oscillations, $T_{sp} = 4$ ms,

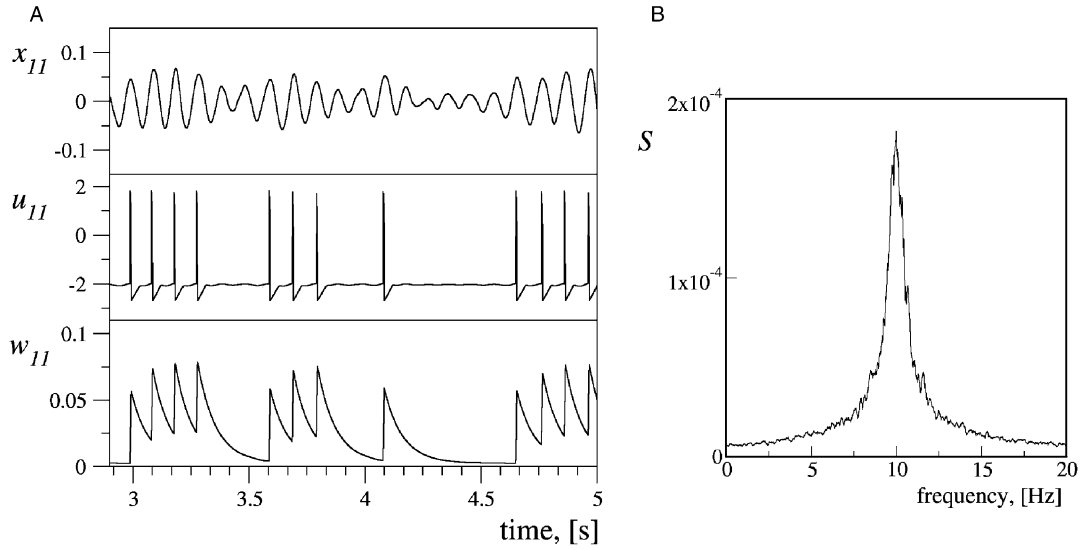


Fig. 2. Noise-sustained oscillations in a unit of the IO lattice (Ia) and response of corresponding units in Axon (Ib) and CN (II) layers (uncoupled case, $d = 0$). (A) Examples of time realization of quasi-monochromatic noise (QMN), $x_{11}(t)$ (top), spiking behavior of the variable $u_{11}(t)$ (middle) and pulse train for $w_{11}(t)$ (bottom); (B) corresponding power spectrum of QMN ($\omega_0 = 2\pi \times 10$, $\gamma = 2$, $I_0 = 2.03$, $D = 0.003$).

which strongly depended on the variable $x(t)$. Namely, spikes appear near maxima of $x(t)$ when neurons overtake the threshold value in Eq. (4). Thus, the stochastic process modeled by Eq. (9) brings rhythmicity to axon firing forcing the generation of spikes with proper timing. In turn the short spikes in the axon excite pulses with duration about 30 ms in the corresponding unit in the CN lattice. If spikes follow with short ISI then the variable w does not have time to recover, the next pulse starts from nonzero amplitude and, consequently, it is a bit higher.

For nonzero electrical coupling between units in the master lattice (Ia) we expect that IO neurons will be able to synchronize their oscillations and, consequently, initiate synchronous activity in the slaved (second) lattice (Ib). However, the synchronization cannot be perfect due to the noisy origin of the oscillations. Thus, we expect to observe imperfect synchronization of spike trains recorded from different units in the Axon lattice (Ib). For nonzero coupling between IO neurons ($d \neq 0$) Eq. (9) becomes

$$\ddot{x}_{jk} + 2\gamma\dot{x}_{jk} + \Omega_0^2 x_{jk} = 2d[(\Delta\dot{x})_{jk} + \gamma(\Delta x)_{jk}] - d^2(\Delta(\Delta x)_{jk})_{jk} + \sqrt{2\omega_0^2 D}\xi_{jk}(t), \quad (13)$$

where to simplify notation we use the discrete Laplace operator:

$$(\Delta x)_{jk} = (\Delta x)_j + (\Delta x)_k, \quad (14)$$

with

$$(\Delta x)_j = x_{j-1k} - 2x_{jk} + x_{j+1k},$$

$$(\Delta x)_k = x_{jk-1} - 2x_{jk} + x_{jk+1}.$$

Stochastic oscillations in the lattice (13) have a chance to synchronize for some time intervals due to the coupling terms in the RHS of Eq. (13).

Before we proceed with the whole Eq. (13) let us consider the simplest case, when the lattice consists of two units only. Then introducing two new variables $s = x_2 - x_1$ and $r = x_2 + x_1$, we get from Eq. (13)

$$\ddot{s} + 2(\gamma + 2d)\dot{s} + (\Omega_0^2 + 4d\gamma)s = \sqrt{4\omega_0^2 D}\xi_s(t), \quad (15)$$

$$\ddot{r} + 2\gamma\dot{r} + \Omega_0^2 r = \sqrt{4\omega_0^2 D}\xi_r(t),$$

where $\xi_s = (\xi_1 - \xi_2)/\sqrt{2}$, and $\xi_r = -(\xi_1 + \xi_2)/\sqrt{2}$ are new independent noise sources with correlation function $\langle \xi_{s,r}(t)\xi_{s,r}(t') \rangle = \delta(t - t')$. Eqs. (15) are independent, and similar to Eq. (9) for a single unit. Using the power spectrum (10) we get for processes x (for $d = 0$), r and s , respectively,

$$\langle x^2 \rangle = \frac{\omega_0^2 D}{2\gamma\Omega_0^2}, \quad \langle r^2 \rangle = \frac{\omega_0^2 D}{\gamma\Omega_0^2}, \quad (16)$$

$$\langle s^2 \rangle = \frac{\omega_0^2 D}{(\gamma + 2d)(\Omega_0^2 + 4d\gamma)}.$$

For high values of the coupling the mean square displacement of the difference variable, s , tends to zero, i.e. oscillations in both units become synchronized. The standard deviation, i.e. the average amplitude of oscillations, for processes $x_1(t)$ and $x_2(t)$, which is the value $\sigma_x = \frac{1}{2}\sqrt{\langle r^2 \rangle + \langle s^2 \rangle}$, is lower than the standard deviation for a single unit and decreases where the value of the coupling coefficient, d , increases. For large values of d

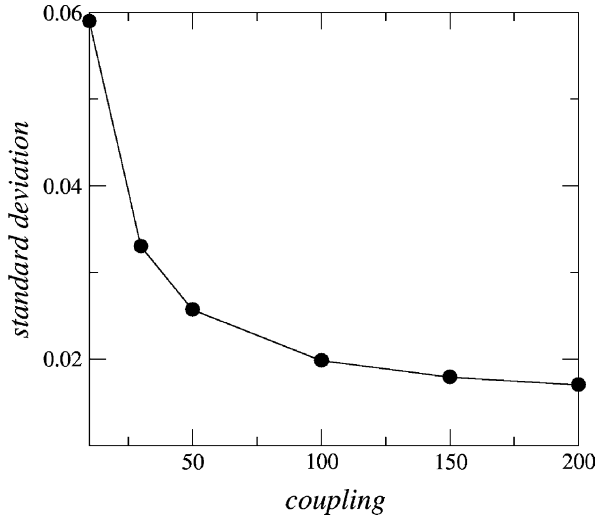


Fig. 3. Standard deviation of the process $x(t)$ (average oscillation amplitude in the IO-layer (Ia)) as a function of coupling strength, d , for fixed value of the noise intensity $D = 0.2$ in the (15×15) IO lattice ($\omega_0 = 2\pi \times 10$, $\gamma = 2$).

the quantity σ_x approaches the value $\sqrt{\langle x^2 \rangle} / 2$. Thus besides their synchronizing role, the coupling terms in Eq. (13) act like additional damping and the resulting oscillations have lower mean amplitude than for $d = 0$. Using Eq. (16) we

can calculate the cross-correlation function for the processes $x_1(t)$ and $x_2(t)$

$$C_x = 1 - \frac{\gamma \Omega_0^2}{\Omega_0^2(\gamma + d) + 2d\gamma(\gamma + 2d)}. \quad (17)$$

For $\Omega_0^2 \gg d\gamma$, from Eq. (17) we obtain $C_x \approx 1 - \frac{\gamma}{\gamma + d}$. Thus to get highly correlated oscillations for $x_1(t)$ and $x_2(t)$ we require that $d \gg \gamma$ (damping is small compared to the coupling between elements in Ia) and, finally, we obtain highly coherent spike trains for $u_1(t)$ and $u_2(t)$.

To check the aforementioned results with the whole lattice, we have made several numerical integrations with different values of the coupling coefficient d . Fig. 3 shows the standard deviation, σ_x , of oscillations in the Ia lattice as a function of the coupling coefficient. As we have seen for the case of two units, the standard deviation decreases with the increase of d . However, due to the higher number of bonds involved and the collective dynamics in the lattice, the standard deviation of oscillations in the IO decays faster than for two units. The value of the average amplitude (standard deviation) controls the spiking activity of the slaved (Axon) lattice Ib. For higher values of σ_x , events such that x_{jk} crosses the threshold, $(I_0 - a)$, in Eq. (3) become more probable. Consequently, spikes appear more frequently. For $I_0 - a = \sigma_x$, in a first approximation, events

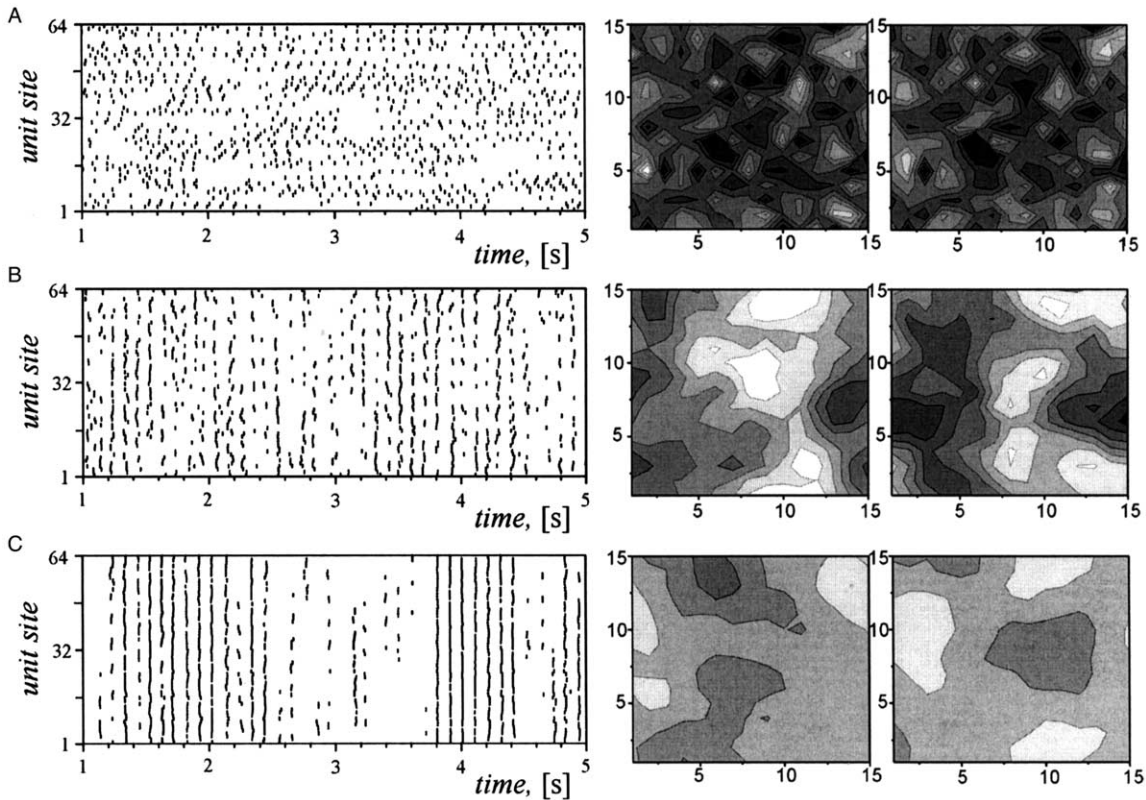


Fig. 4. Picrotoxin-like effect for different values of coupling between IO neurons with fixed value of $\sigma_x = 0.026$ controlled by the noise intensity. (A) Vanishing coupling $d = 0$, $D = 0.003$; (B) Intermediate coupling $d = 50$, $D = 0.2$; (C) Strong coupling $d = 200$, $D = 0.55$. Spatiotemporal evolution of the oscillations in the (Ib) Axonal layer (left panels). A (8×8) -square part of the (15×15) -lattice is shown on the raster displays. Each vertical black bar corresponds to a spiking event in a given unit. Two successive snapshots (right panels) with $\Delta t = 100$ illustrate oscillations in the (Ia) IO-layer. Gray intensity is proportional to the value of x .

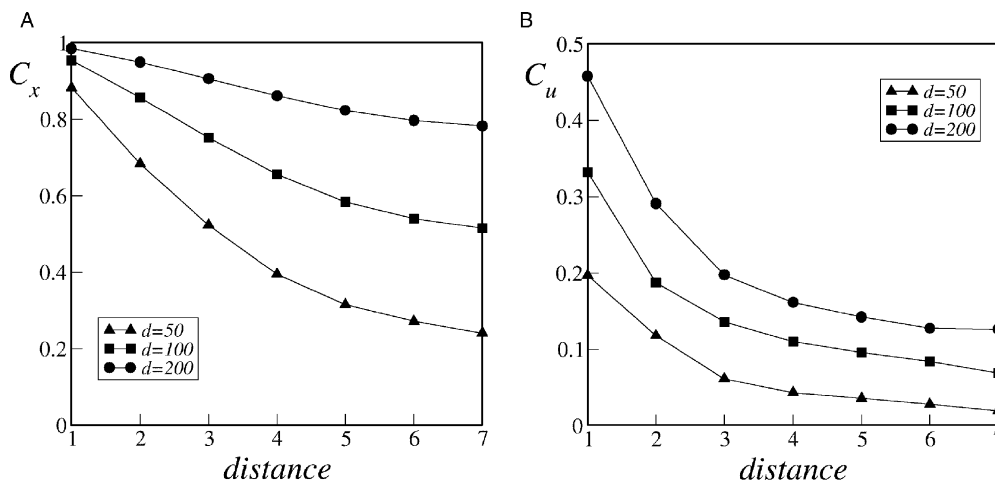


Fig. 5. Cross-correlation functions calculated using Eq. (12) with time averaging and following averaging over a lattice for different values of inter-layer coupling coefficient, d : (A) for the IO lattice (Ia), (B) for the Axon lattice (Ib).

with $x(t)$ maxima above or below the value σ_x are equiprobable and hence the average number of spikes is one in two periods of $x(t)$. To avoid difference in spiking activity for different values of d we tune the noise intensity, $D = D(d)$, so that σ_x remains constant. Fig. 4 summarizes the results of such computations. Clearly, the oscillations both in the IO lattice (Ia) and in the Axon layer (Ib) have moderate level of coherence for $d = 50$ and a high level for $d = 200$ (Fig. 4b and c) relative to the case $d = 0$. Fig. 5 shows cross-correlation functions for several different values of the coupling strength. For $d = 200$ (Fig. 4c) almost all units in the IO layer (Ia) belong to few transient clusters where elements oscillate together for a while. Such clusters randomly drift over the lattice. Due to the synchronous oscillations in the IO (Ia) we observe coherent spikes in the Axon layer (Ib). However, from time to time the oscillation amplitudes drastically decrease and clusters break through the phenomenon of phase resetting earlier mentioned (Nekorkin, Makarov, & Velarde, 1998; Tass, 1999). This leads to silent behavior in the Axon lattice during several periods (Fig. 4b and c). Then units in the IO lattice reorganize, their oscillation amplitudes grow and new spike trains appear in the Axon lattice (Ib).

4. Restrictions to cluster growth due to the feedback loop

Let us now consider the three-layer system with closed feedback loop ($\Gamma \neq 0$) and, in the general case, when the coupling coefficients between IO neurons in lattice Ia are not constant. As already mentioned each coupling between units in the IO lattice can be altered by the signals activated by the neurons, which are linked by this coupling. The signals pass via Axons to CN and finally decrease the coupling coefficient due to Eq. (8). The upper two diagrams of Fig. 6 show pulse trains in two neighboring neurons with indexes (11) and (12) in the CN lattice (II) activated by spikes coming from the Axon layer (Ib) and the lower

diagram of Fig. 6 shows the evolution of the coupling coefficient between the original IO (Ia) neurons with indexes (11) and (12). Each pulse, due to Eq. (8), reduces value of the coupling coefficient between IO neurons while it lasts. Thus the average coupling between neurons is lower than for vanishing Γ , as discussed in Section 3. Consequently, the coherence level of oscillations in the IO layer (Ia) and spike trains in the Axon layer (Ib) will be smaller for the same parameter values.

Besides the decoupling coefficient, Γ , the value of the hyperpolarizing current, I_0 , should significantly influence the evolution of the system. In experiments, harmaline injection leads to a decrease in spiking activity (the average spike rate) of PC (and axons), but spike trains become more

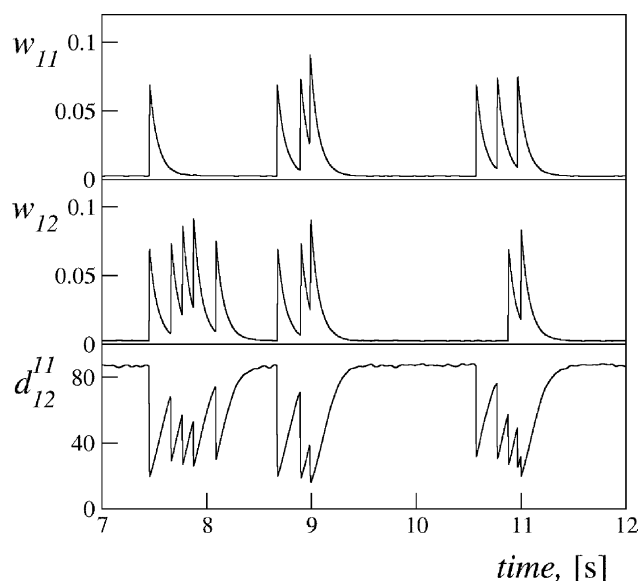


Fig. 6. Illustration of the influence of the (CN–IO) feedback loop on the intra-layer coupling coefficient between IO neurons with indexes (11) and (12) in lattice Ia. The sequence of pulses in two neighboring units in the (II) CN lattice (top and middle panels), and resulting coupling coefficient d_{12}^{11} between corresponding neurons in the (Ia) IO lattice (bottom).

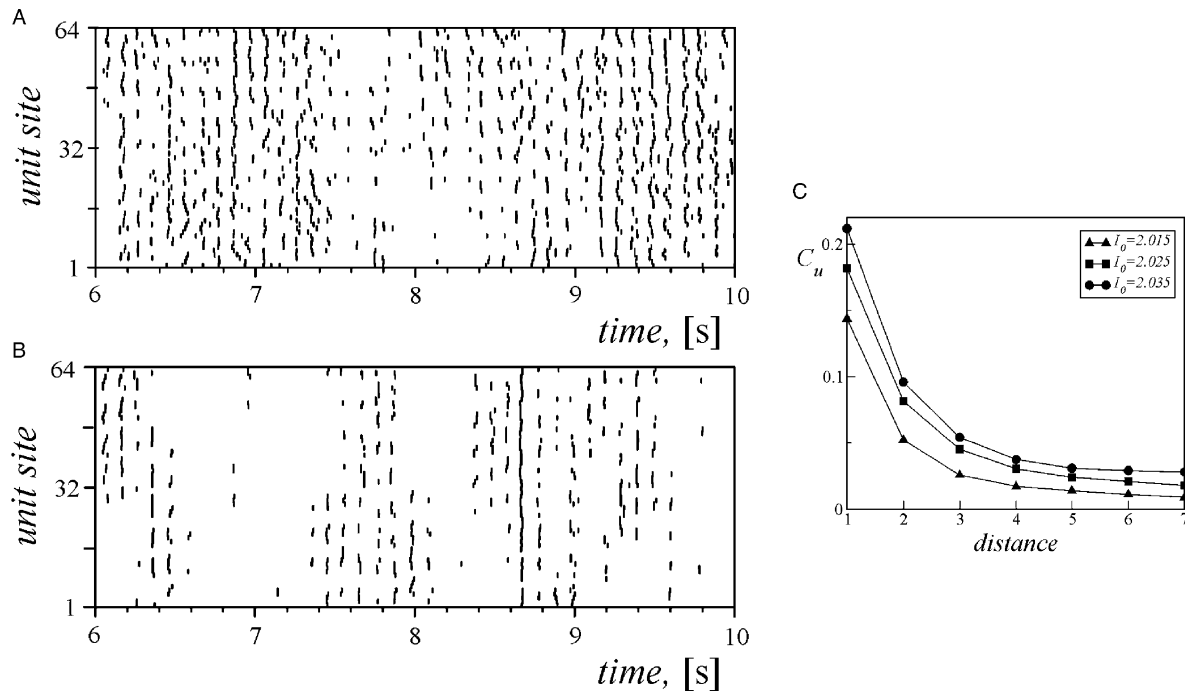


Fig. 7. Illustration of the influence of the hyperpolarizing current, I_0 , on the coherence of spike trains in the Axonal lattice (Ib) with operating feedback (CN–IO) loop. (A) $I_0 = 2.025$; (B) $I_0 = 2.035$; (C) Cross-correlation function of spike trains in the Axonal lattice (Ib) for three different values of I_0 .

coherent. To test our model for its ability to account for this experimental fact we have made several computations with different values of I_0 . Fig. 7 shows two examples of spike trains in the Axon layer (Ib) on the raster display and cross-correlation functions for different values of I_0 . As expected,

the spiking activity for low level of hyperpolarizing current ($I_0 = 2.025$ in Fig. 7a) is higher than for higher levels of the current ($I_0 = 2.035$ in Fig. 7b). There is less correlation between units in the first case (Fig. 7c). This phenomenon can be explained in the following way. An increase of

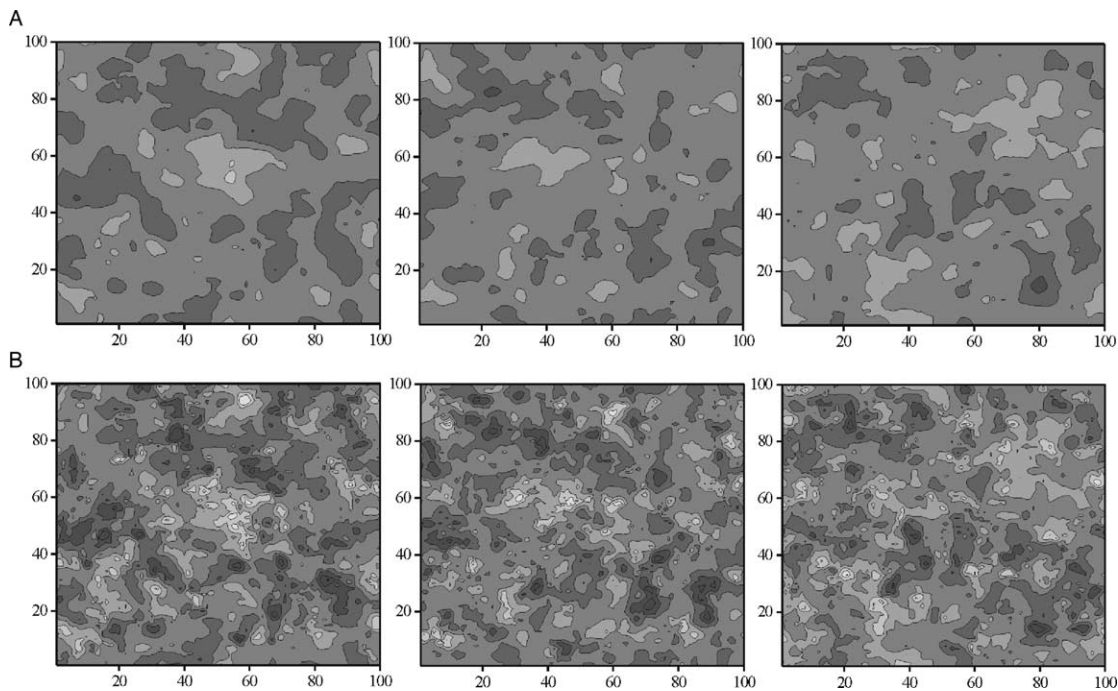


Fig. 8. Illustration of the restriction on cluster size in the (100×100) IO lattice due to control feedback loop via the CN lattice. Three successive snapshots with $\Delta t = 100$ ms (color corresponds to the value of x) (A) without feedback loop, $\Gamma = 0$; (B) with operating feedback loop, $\Gamma = 30$ ($d = 200$, $D = 0.55$, $I_0 = 2.03$).

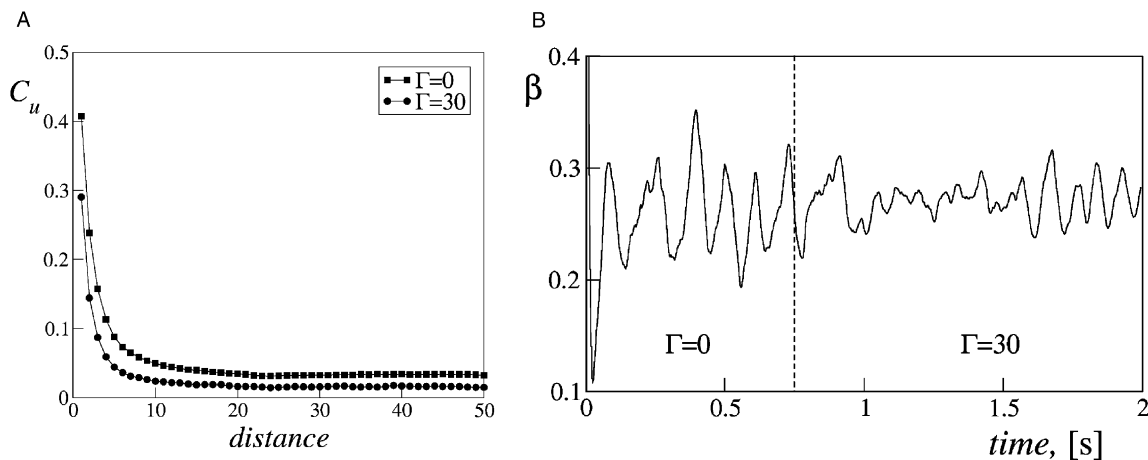


Fig. 9. Characteristics of oscillations in a large (100×100) system for different coupling regimes (without feedback loop, $\Gamma = 0$, and with feedback loop, $\Gamma = 30$). (A) Cross-correlation functions for spike trains in the Axonal lattice (Ib); (B) Markov parameter β , calculated for oscillations in the IO lattice (Ia), as a function of time. In a first stage (left of the dashed vertical line) the intra-layer coupling is constant, and no feedback mechanism is involved $\Gamma = 0$. In the second stage (right of the dashed line) the feedback loop is operating, $\Gamma = 30$. All other parameter values and conditions are the same as in Fig. 8.

hyperpolarizing level, I_0 , leads to a lower probability in the appearance of spikes in the Axon lattice (Ib) since the probability is a monotonically increasing function of

$$\sigma_x - (I_0 - a). \quad (18)$$

Thus the spiking activity decreases with increasing values of I_0 (down to zero for $I_0 \rightarrow \infty$). Then in the CN lattice pulses formed by the spikes become rare that leads to higher mean values of the coupling coefficients in the IO layer. Since the coherence level is higher for high coupling values (see Fig. 5b), we get more correlated spike trains in the Axon layer (Ib). Then, a higher coupling, due to its damping character, decreases the mean oscillation amplitude, σ_x , and the spiking activity further diminishes due to Eq. (18). This process eventually reaches a saturation level and, finally, we have stationary oscillations with rare albeit more coherent spikes in the Axon lattice (Ib).

Finally, we have carried out computations with rather large (100×100) lattices. This allows us to estimate the so-called Markov parameter β for the IO layer allowing comparison with experimental results (Makarenko, Welsh, Lang, & Llinas, 1997). This parameter estimates how much a given spatial distribution differs from the uniform one. If no statistically reliable difference exists then $\beta \rightarrow 0$. Fig. 8 shows several successive snapshots of the oscillations in the IO lattice (Ia) without ($\Gamma = 0$) and with ($\Gamma \neq 0$) feedback loop. In both cases we observe, as a result of synchronization, clusters of neurons oscillating together (the same gray intensity in Fig. 8). The boundaries of the clusters in the lattice Ia change in time and clusters erratically wander over the lattice. However, the average size of the clusters with feedback loop ($\Gamma \neq 0$) is smaller than with constant coupling. Besides, the boundaries between clusters are ‘clearer’ (the gradient of gray is higher). This occurs due to ‘self tuning’ of bonds between units inside and outside a cluster, which is impossible with a constant coupling

coefficient ($\Gamma = 0$). Generally, the coupling between units deep inside a cluster is stronger than between units at the boundary of clusters. Thus the feedback loop, via the CN lattice, not only helps breaking and recreating clusters in the IO lattice preventing their uncontrolled growth but also makes them ‘brighter’. This makes the time lag of the coherence of spikes in the Axon lattice (Ib) smaller when the feedback loop operates (Fig. 9a). The Markov parameter, β , reflects an important consequence of the negative feedback for the system. Its standard deviation is significantly lower when the feedback is activated. This means that the system is kept at a particular level of spatial organization with specific number of degrees of freedom.

5. Conclusions

We have studied the time evolution of a three-layer mathematical model that adequately simulates the qualitative dynamics of cluster formation, reorganization and spike-train generation in the Olivo-Cerebellar system. We have restricted the study of the model to the autonomous functioning of the system (without external input signals like those arising from sensory- and moto- neurons) because a considerably more complex behavior is expected in the presence of external input, which requires a separate study. The model incorporates the (excitatory) feedforward and (inhibitory) feedback loops as it is known to occur with IO neurons, collateral axons (related, indeed, to the PC layer), and CN. Unavoidable noise always existing in neurobiological systems is taken into account not just as an accessory element affecting the dynamics, but for the purpose of adequately using the simplest mathematical oscillator, the harmonic oscillator. Indeed, the (white additive) noise helps sustaining subthreshold oscillations. When dissipation in such an oscillator is small and hence its

time scale is much larger than the oscillation period, the outcome is a quasi-monochromatic (colored) noise. Its spectrum has a well-defined peak at the frequency 10 Hz, and the waveform is similar to the subthreshold oscillations observed in IO neurons. Although the nature of the model subthreshold oscillation is stochastic, it brings rhythmicity to axon firing forcing the generation of spike trains with time structure of the underlying oscillations (the interspike histogram shows pronounced peaks at multiples of 100 ms). Every time there is a spike in an axon, there appears a pulse in the CN lattice leading to a reduction of the strength and/or number of connections between an IO neuron and its neighbors. Depending on the strength of bonds (gap-junctions) in the IO base layer different patterns of synchronous activity (clusters of different sizes) can appear. IO neurons will be able to synchronize their oscillations and, consequently, initiate synchronous activity in the feed-forward lattices.

The qualitative behavior of the model explains well the features observed in experiments with IO neurons and also allows making further significant predictions, amenable to experimental test. We have studied the dynamics of the model with and without inhibitory CN–IO feedback. The latter case simulates the pharmacological intervention with picrotoxin or lesion of CN in *in vivo* experiments. In the absence of feedback the network shows synchronous activity with larger and larger clusters as the coupling strength increases. However, the synchronization cannot be perfect due to the noisy origin of the oscillations. Thus, we observe imperfect synchronization of spike trains recorded from different units in the Axon lattice. Eventually the oscillation amplitudes drastically decrease thus allowing fast ‘switching’ of oscillation phases and, hence clusters split in a phase resetting process. This leads to silent behavior in the Axon lattice during several periods. Then units in the IO lattice reorganize into new clusters, their oscillation amplitudes grow again and new spike trains appear in the Axon lattice. This is also in agreement with experimental data.

Computations for two units show that a high coupling strength between units results in highly coherent oscillations and spiking, but the increase in the coupling also decreases the mean amplitude of (subthreshold) oscillations. Thus besides the synchronizing role, the bonds act like additional damping and the resulting oscillations have lower mean amplitude. These two features are also found in experiments (Benardo & Foster, 1986). If the (inhibitory) feedback is present the synchronization in the network is drastically reduced and clusters become smaller in size. Spikes in an axon via the CN lattice reduce the strength of bonds or couplings between IO neurons. As the average coupling strength is reduced the coherence level is also reduced.

Increasing the hyperpolarization level of the IO neurons we found a decrease in the firing rate, as expected, and a less obvious increase in the coherence level of the spikes. This is what happens in experiments with IO neurons using harmaline (Llinas, 1989; Sasaki et al., 1989; Yamamoto

et al., 2001). For strong hyperpolarization, firing events occur less frequently when both oscillation amplitudes of *all* pairs of neighboring units are high and oscillation phases are close (otherwise it is difficult to go above threshold). Then in the CN lattice pulses formed by the axon spikes become rare. This leads to less significant damping effect of the couplings by the inhibitory feedback and, consequently, the mean coupling values in the IO layer increases. Since the coherence level is higher for high coupling values more correlated spike trains are observed in the Axon layer. Then, higher values of the coupling strength, due to its damping character, decrease further the mean oscillation amplitude. Consequently, there is further improvement of the coherence level until saturation is reached. Besides, the boundaries between clusters become sharper due to the enhancement (via feedback) of the coupling strength inside a cluster relative to its environment. Uncoupled signals from CN are less frequent for the synchronously firing neurons (in one cluster) than for those firing out of phase (in different clusters). Hence the coupling between units deep inside a cluster is stronger than between units at the boundary of clusters. Thus the feedback loop, via the CN lattice, not only helps breaking and recreating clusters in the IO lattice preventing their uncontrolled growth but also makes them ‘brighter’. Finally, in the case when the inhibitory CN–IO feedback loop is operating ($I \neq 0$) a decrease is predicted for the standard deviation of the Markov parameter, β , discriminating a pattern from homogeneous random distribution.

The study presented here offers ground for future work. For instance, the model could be extended by using more sophisticated model neurons (like robust nonlinear oscillators without or with noise) and more accurate (intralayer) IO neuron bonds. One can also have more complexity in the model of axons and other interlayer (IO–PC–CN) couplings by adding delays, or take into account external inputs thus incorporating other parts of the cerebellar related circuitry, all together leading to a useful tool to test motor-control mechanisms. Note that if external stimuli are added, the PC layer is expected to play an important role and its dynamics has to be explicitly included in the model. This layer will modulate (in accordance to the input signal) the inhibitory feedback to IO in such a way that clusters of synchronous activity associated with a specific movement may be increased (stabilized) during the movement, while ‘not-desirable’ clusters could be suppressed. This needs the system to be highly responsive and ready for fast cluster reorganization that, in our view, may happen via appropriate blocking of gap-junctions like the present study predicts.

Acknowledgements

The authors acknowledge fruitful discussion with Dr E. Lang and Dr J. Welsh. This work was supported by

a Grant from the BCH Foundation (Spain), by the Spanish Ministry of Science and Technology under Grant PB 96-599, by the National Institutes of Health/National Institute of Neurological Disorders and Stroke Grant NS13742 and by the U.S. Department of Defense/Office of Naval Research Grant N00149911081.

References

- Armstrong, D. M., Eccles, J. C., Harvey, R. J., & Matthews, P. B. C. (1968). Responses in the dorsal accessory olive of the cat to stimulation of hindlimb afferents. *Journal of Physiology*, *194*, 125–145.
- Bal, T., & McCormick, D. A. (1997). Synchronized oscillations in the inferior olive are controlled by the hyperpolarization-activated cation current I_h . *Journal of Neurophysiology*, *77*, 3145–3156.
- Baltanas, J. P., & Casado, J. M. (1998). Bursting behavior of the FitzHugh-Nagumo neuron model subject to quasi-monochromatic noise. *Physica D*, *122*, 231–240.
- Bell, C. C., & Kawasaki, T. (1972). Relations among climbing fiber responses of nearby Purkinje cells. *Journal of Neurophysiology*, *35*, 155–169.
- Benardo, L. S., & Foster, R. E. (1986). Oscillatory behavior in inferior olive neurons: mechanism, modulation, cell aggregates. *Brain Research Bulletin*, *17*, 773–784.
- Bower, J., & Llinas, R. (1982). Simultaneous sampling and analysis of the activity of multiple, closely adjacent cerebellar Purkinje cells. *Society for Neuroscience Abstracts*, *8*, 830.
- Campbell, S. A., Belair, J., Ohira, T., & Milton, J. (1995). Limit cycles, tori, and complex dynamics in a second-order differential equation with delayed negative feedback. *Journal of Dynamics and Differential Equations*, *7*, 213–236.
- Chan-Palay, V., & Palay, S. L. (1971). Tendril and glomerular collaterals of climbing fibers in the granular layer of the rat's cerebellar cortex. *Journal Anatomie Entwicklungsgesch.*, *133*, 247–273.
- Cronin, J. (1987). *Mathematical aspects of Hodgkin–Huxley neural theory*. Cambridge: Cambridge University Press.
- Doi, S., Inoue, J., Sato, S., & Smith, C. E. (1999). Bifurcation analysis of neuronal excitability and oscillations. In R. R. Poznanski (Ed.), *Modeling in the Neurosciences. From ionic channels to neural networks*. Switzerland: Harwood Academic Publisher, Chapter 16.
- Eccles, J. C., Llinas, R., & Sasaki, K. J. (1966). The excitatory synaptic action of climbing fibers on the Purkinje cells of the cerebellum. *Journal of Physiology (London)*, *182*, 268–296.
- Fitz Hugh, R. (1961). Impulses and physiological states in theoretical models of nerve membrane. *Biophysical Journal*, *1*, 445–466.
- Fukuda, M., Yamamoto, T., & Llinas, R. R. (1987). Simultaneous recordings from Purkinje cells of different folia in the rat cerebellum and their relation to movement. *Society for Neuroscience Abstracts*, *13*, 603.
- Fukuda, M., Yamamoto, T., & Llinas, R. R. (2001). The isochronic band hypothesis and climbing fiber regulation of motricity: an experimental study. *European Journal of Neuroscience*, *13*, 315–326.
- Gardiner, G. W. (1985). *Handbook of stochastic methods for physics, chemistry and the natural sciences* (2nd ed.). New York: Springer.
- Giaquinta, A., Argentina, M., & Velarde, M. G. (2000). A simple generalized excitability model mimicking salient features of neuron dynamics. *Journal of Statistical Physics*, *101*, 665–678.
- Gottlieb, D. I. (1988). In R. R. Llinas (Ed.), *GABAergic Neurons. The biology of the brain. From neurons to networks*, New York: W.H. Freeman and company.
- Haken, H. (1996). *Principles of brain functioning. A synergetic approach to brain activity, behavior and cognition*. Berlin: Springer.
- Holden, A. V. (1976). *Models of the stochastic activity of neurons*. Berlin: Springer.
- Hoppensteadt, F. C. (1986). *An Introduction to the mathematics of neurons*. Cambridge: Cambridge University Press.
- Izhikevich, E. M. (2000). Neural excitability, spiking and bursting. *International Journal Bifurcation and Chaos*, *10*, 1171–1266.
- Lamarre, Y., de Montigny, C., Dumont, M., & Weiss, M. (1971). Harmaline induced rhythmic activity of cerebellar and lower brain stem neuron. *Brain Research*, *32*, 246–250.
- Lampf, I., & Yarom, Y. (1997). Subthreshold oscillations and resonant behavior: two manifestations of the same mechanism. *Neuroscience*, *78*, 325–341.
- Lang, E. J., Sugihara, I., & Llinas, R. R. (1996). GABAergic modulation of complex spike activity by the cerebellar nucleoolivary pathway in rat. *Journal of Neurophysiology*, *76*, 255–275.
- Latham, A., & Paul, D. H. (1971). Spontaneous activity of cerebellar Purkinje cells and their response to impulses in climbing fibers. *Journal of Physiology (London)*, *212*, 135–156.
- Lee, S. G., Neiman, A., & Kim, S. (1998). Coherence resonance in a Hodgkin–Huxley neuron. *Physical Review E*, *57*, 3292–3297.
- Llinas, R. R. (1989). In S. Piergiorgio (Ed.), *Electrophysiological properties of the olivocerebellar system. The olivocerebellar system in motor control*, Berlin: Springer.
- Llinas, R., Baker, R., & Sotelo, C. (1974). Electrotonic coupling between neurons in cat inferior olive. *Journal of Neurophysiology*, *37*, 560–571.
- Llinas, R. R., & Sasaki, K. (1989). The functional organization of the olivocerebellar system as examined by multiple purkinje cell recordings. *European Journal of Neuroscience*, *1*, 587–602.
- Llinas, R. R., & Simpson, J. I. (1981). Cerebellar control of movement. In A. L. Towe, & E. S. Luschei (Eds.), *Handbook of behavioral neurobiology*, *5, motor coordination* (pp. 231–302). New York: Plenum press.
- Llinas, R. R., & Volkind, R. A. (1973). The olivo-cerebellar system: functional properties as revealed by harmaline-induced tremor. *Experimental Brain Research*, *18*, 69–87.
- Llinas, R. R., & Yarom, Y. (1981a). Electrophysiology of mammalian inferior olivary neuron in vitro. Different types of voltage-dependent ionic conductances. *Journal of Physiology*, *315*, 549–567.
- Llinas, R. R., & Yarom, Y. (1981b). Properties and distribution of ionic conductances generating electroresponsiveness of mammalian inferior olivary neurons in vitro. *Journal of Physiology*, *315*, 569–584.
- Llinas, R. R., & Yarom, Y. (1986). Oscillatory properties of guinea-pig inferior olivary neurons and their pharmacological modulation: an in vitro study. *Journal of Physiology (London)*, *376*, 163–182.
- Llinas, R. R., & Welsh, J. P. (1993). On the cerebellum and motor learning. *Current Opinions in Neurobiology*, *3*, 958–965.
- Longtin, A. (1997). Autonomous stochastic resonance in bursting neurons. *Physical Review E*, *55*, 868–876.
- MacDonald, N. (1989). *Biological delay systems: linear stability theory*. Cambridge: Cambridge University Press.
- Makarov, V. A., Nekorkin, V. I., & Velarde, M. G. (2001). Spiking behavior in a noise-driven system combining oscillatory and excitatory properties. *Physical Review Letters*, *86*, 3431–3434.
- Makarenko, V. I., & Llinas, R. (1998). Experimentally determined chaotic phase synchronization in neuronal system. *Proceedings of National Academy of Sciences (USA)*, *95*, 15747–15752.
- Makarenko, V. I., Welsh, J. P., Lang, E. J., & Llinas, R. (1997). A new approach to the analysis of multidimensional neuronal activity: Markov random fields. *Neural Networks*, *10*, 785–789.
- Manganaro, G., Arena, P., & Fortuna, L. (1999). *Cellular neural networks. Chaos, complexity and VLSI processing*. Berlin: Springer.
- Manor, Y., Rinzel, J., Segev, I., & Yarom, Y. (1997). Low-amplitude oscillations in the inferior olive: a model based on electrical coupling of neurons with heterogeneous channel densities. *Journal Neurophysiology*, *77*, 2736–2752.
- Mikhailov, A. S., & Calenbuhr, V. (2002). *From cells to societies. Models of complex coherent action*. New York: Springer.

- de Montigny, C., & Lamarre, Y. (1973). Rhythmic activity induced by harmaline in the olivo-cerebello-bulbar system of the cat. *Brain Research*, 53, 81–95.
- Mugnani, E., & Oertel, W. H. (1981). Distribution of glutamate decarboxylase-positive neurons in the rat cerebellar nuclei. *Society of Neuroscience Abstracts*, 7, 122.
- Nekorkin, V. I., Makarov, V. A., & Velarde, M. G. (1998). Clustering and phase resetting in a chain of bistable nonisochronous oscillators. *Physical Review E*, 58, 5742–5747.
- Nekorkin, V. I., & Velarde, M. G. (2002). *Synergetic phenomena in active lattices. Patterns, waves, solitons, chaos*. Berlin: Springer.
- Nelson, B. J., Barmack, N. H., & Mugnani, E. (1984). A GABAergic cerebello-olivary projection in the rat. *Society Neuroscience Abstracts*, 10, 539.
- Olien, L., & Belair, J. (1997). Bifurcations, stability and monotonicity properties of a delayed neural network model. *Physica D*, 102, 349–363.
- Pikovsky, A. S., & Kurths, J. (1997). Coherence resonance in a noise-driven excitable system. *Physical Review Letters*, 78, 775–778.
- Ruigrok, T. J. (1997). Cerebellar nuclei: the olivary connection. *Progress in Brain Research*, 114, 167–1992.
- Sasaki, K., Bower, J. M., & Llinas, R. R. (1989). Multiple purkinje cell recordings in rodent cerebellar cortex. *European Journal of Neuroscience*, 1, 572–586.
- Sasaki, K., & Llinas, R. R. (1985). Dynamic electronic coupling in mammalian inferior olive as determined by simultaneous multiple purkinje cell recording. *Ebiophysical Journal*, 47, 53a.
- Schweighofer, N., Doya, K., & Kawato, M. (1999). Electrophysiological properties of inferior olive neurons: a compartmental model. *Journal of Neurophysiology*, 82, 804–817.
- Sotelo, C., Gotow, T., & Wassef, M. (1986). Localization of glutamic-acid decarboxylase immunoreactive axon terminals in the inferior olive of the rat, with special emphasis on anatomic relations between GABAergic synapses dendrodendritic gap junctions. *Journal of Comparative Neurology*, 252, 32–50.
- Sotelo, C., Llinas, R., & Baker, R. (1974). Structural study of inferior olivary nucleus of the cat: morphological correlates of electrotonic coupling. *Journal of Neurophysiology*, 37, 541–559.
- Sugihara, I., Lang, E. J., & Llinas, R. (1993). Uniform olivocerebellar conduction time underlies Purkinje cell complex spike synchronicity in the rat cerebellum. *Journal of Physiology (London)*, 470, 243–271.
- Szentagothai, J., & Rajkovits, K. (1959). Ueber den ursprung der kletterfasern des kleinhirns. *Journal Anatomie Entwicklungsgesh*, 121, 130–141.
- Tass, P. A. (1999). *Phase resetting in medicine and biology. Stochastic modeling and data analysis*. Berlin: Springer.
- Tuckwell, H. C. (1989). *Stochastic processes in the neurosciences. Society for industrial and applied mathematics (SIAM)*.
- Vallbo, A. B., & Wessberg, J. (1993). Organization of motor output in slow finger movements in man. *Journal of Physiology (London)*, 469, 673–691.
- Velarde, M. G., Nekorkin, V. I., Kazantsev, V. B., Makarenko, V. I., & Llinas, R. R. (2002). Modeling inferior olive neuron dynamics. *Neural Networks*, 15, 5–10.
- Wei, J., Velarde, M. G., & Makarov, V. A. (2002). Oscillatory phenomena and stability of periodic solutions in a simple neural network with delay. *Nonlinear Phenomena in Complex Systems*, 5, 407–417.
- Welsh, J. P., Lang, E. J., Sugihara, I., & Llinas, R. (1995). Dynamic organization of moto control within the olivocerebellar system. *Nature (London)*, 374, 453–457.
- Welsh, J. P., & Llinas, R. R. (1997). In C. I. De Zeeuw, P. Strata, & J. Voogol (Eds.), *Some organizing principles for the control of movement based on olivocerebellar physiology (vol. 114)* (pp. 449–461). *Progress in Brain Research*, New York: Elsevier, Chapter 23.
- Yamamoto, T., Fukuda, M., & Llinas, R. R. (2001). Bilaterally synchronous complex spike Purkinje cell activity in the mammalian cerebellum. *European Journal of Neuroscience*, 13, 327–339.
- Yarom, Y., & Llinas, R. R. (1987). Long-term modifiability of anomalous and delayed rectification in guinea pig inferior olivary neurons. *Journal of Neuroscience*, 7, 1166–1177.
- Yarom, Y. (1989). Oscillatory behavior of olivary neurons. In P. Strata (Ed.), *The olivo-cerebellar system in motor control (vol. 17)* (pp. 209–220). *Experimental Brain Research Series*, Berlin: Springer.